HETEROGENEOUS CATALYSIS USING BENTONITE-SUPPORTED Fe-Co-Ni TRIMETALLIC NANOPARTICLES

ADERIBIGBE FATAI ALADE[1]*, ADEWOYE TUNMISE LATIFAT[1], MUSTAPHA SHERIF ISHOLA[1], MOHAMMED ISHAQ ALHASSAN[1], SAKA HARVIS BAMIDELE[2], AJALA ELIJAH OLAWALE[1], OLUWASEYI SOILE SAMUEL[1]

[1] *Department of Chemical Engineering, Faculty of Engineering and Technology, University of Ilorin, Ilorin, Nigeria*

[2] *Quality Control Department, Segmax Oil Nigeria Limited, Kere-Aje, Ogbondoroko, Kwara State, Nigeria*

Abstract: Herein, the synthesis and characterization of a bentonite-supported Fe-Co-Ni trimetallic nanocatalyst applied in transesterification reaction was reported. The synthesized heterogeneous catalyst was used to investigate the production of biodiesel by varying the reaction parameters using Box-Behnken design response surface methodology (RSM-BBD). An optimum biodiesel yield of 95.2 % was obtained at methanol to oil ratio of 10:1, reaction time of 2 hours, reaction temperature of 55 ℃ and catalyst concentration of 5 % (w/w of the oil). The biodiesel produced was later analysed using GC-MS analysis and the results shows a fatty acid methyl esters (FAME) profile that confirms the presence of biodiesel.

Keywords: bentonite, nanocatalyst, biodiesel, trimetallic, heterogeneous catalysis

1. INTRODUCTION

The search for safer, more efficient forms of energy is a continuous process. Among the several sources of energy discovered are renewable and non-renewable energy [1]. Both categories have advantages and disadvantages. For instance, the advantages of a non-renewable source of energy include readily available, relatively cheap and can be easily utilized in the production of electricity, and transportation fuels. Despite these advantages, it is unsustainable in the long run because of some disadvantages associated with it such as its consumption at a faster rate than it can be replaced or reused [2].

Petroleum diesel fuel is an example of non-renewable energy that has been used to power engines of cars, machines as well as electricity turbines. Its utilization has been the source of carbon dioxide and other greenhouse gases that are responsible for the depletion of the ozone layer leading to climate change and global warming [3]. This global warming has made environment inconvenient for plants, animals and humans. Therefore, there is the need to replace these non-renewable fossil fuels with renewable sources that can guarantee environmental sustainability for all.

Renewable energy sources have been considered as alternative sources that can replace non-renewable sources due to the advantages of the former in providing more efficient, eco-friendly and easily replaceable energy sources

* Corresponding author, email: aderibigbe.fa@unilorin.edu.ng

as compared to the latter [4]. Renewable energy sources include solar, wind, hydropower, wave, tidal and biomass energy, and abundant in nature [1]. Some of these renewable energy sources have been exploited over time. In particular, solar, wind and hydroelectric have been studied by several researchers and it has been reported that they are more effective, readily available and environmentally friendly as alternatives or replacements for the fossil-fuels [1].

Biomass material is another important source of renewable energy that has been used in the production of biodiesel through transesterification reactions. It has the potential to replace the diesel produced from petroleum and can be applied for industrial and domestic purposes. Biodiesel is reported as a promising alternative for the use in diesel engines than petroleum produced diesel oil. Despite these advantages, there is still a setback in its application [5]. For instance, its production requires an appropriate choice of triglyceride source, the alcohol and the catalyst. Any deviance in the choice of the reagent may impact negatively its cost of production. Other parameters such as the molar ratio of the triglyceride to the alcohol as well as catalyst dosage also affect the quality and optimum yield of the biodiesel in the course of the production process.

The sources of the triglyceride source are an important parameter as it determines the amount of energy required to convert it into biodiesel. Over the years, researchers have been searching for a better triglyceride source and those from waste cooking oil [6], vegetable oils [7], algal oils [8] and jatropha oil [9] have been investigated. Generally, two sources have been identified which are edible and non-edible sources. The utilization of any of these sources depends on oil composition, oil yield, economic viability, as well as land availability for its cultivation [5]. In terms of the catalytic requirement for transesterification process, three types of catalyst have been identified and they are homogeneous, heterogeneous and enzyme catalyst [10]. Homogeneous catalysts are in the same state as the biodiesel and glycerol formed, which make it difficult to separate, adding extra cost to the process. Heterogeneous catalysts, on the other hand, are in the solid-state and can be easily separated from the final products and can also be reused [11].

Although homogeneous catalysts require additional stages, they give a lower reaction time compared to heterogeneous catalysts. The fact that they are in a liquid state makes them more active and their active sites are mobile, which helps to reduce the reaction time. Longer trans-esterification reaction time observed with the heterogeneous catalysis can be tackled by using more active compound(s) to generate the catalyst and increasing the surface area. Catalysts generated using transition metals such as Iron (Fe), nickel (Ni), and cobalt (Co) have been reported to be quite active [12]. Another way to reduce the reaction time is to increase surface area by using a nanosized catalyst instead of a microsized catalyst. This increases the number of active sites per surface area on the catalyst thereby reducing the reaction time. Adding a support material also helps increase the surface area of the catalyst.

Several heterogeneous catalysts have been made from transition metals using various support materials such as kaolin [12], alumina [13], silica [14] and $CaCO_3$ [15]. Selecting a good support material for a catalyst in a trans-esterification reaction depends on its properties such as its inertness, its stability and its high surface area [12]. Bentonite is a rock that has a crystalline clay-like mineral and has a wide range of applications in a lot of industries such as the foundry (as moulding sand), agricultural industry, and petroleum industry (as drilling fluid, decolourization process, catalysts) [16]. Bentonite is thermally stable and crystalline; it has a high surface area and high cation-exchange capacity [16]. It is also a naturally existing material which makes it readily available with little or no material preparation stage, therefore, reducing production cost. In addition to its low cost, bentonite has some advantages for use as a support, such as the absence of toxic components and its chemical reactivity which makes it good support to impregnate with the transition metals [17]. Table 1 reveals the chemical composition of standard bentonite.

Table 1. Chemical composition of bentonite [17].

Compound	SiO_2	Al_2O_3	Fe_2O_3	CaO	MgO	K_2O	Na_2O
Amount (%)	70 ± 2.0	14 ± 1.0	1.8 ± 0.2	0.7 ± 0.2	1.7 ± 0.2	1.8 ± 0.2	0.4 ± 0.2

In this study, palm kernel was used as the triglyceride source because it guarantees the quality of biodiesel to be produced which also meets the international standards for biodiesel including ASTM D6751 (US), EN 14214 (Europe) and BIS (India) [18, 19]. Herein, the synthesis of a bentonite-supported Fe-Co-Ni tri-metallic nano-catalyst applied in transesterification reaction is reported. The synthesized catalyst was characterized for its morphology, composition, crystalline nature, thermal stability and functional groups were determined using high resolution scanning electron microscopy (HRSEM), energy dispersion spectroscopy (EDS), x-ray diffraction

(XRD), thermal gravimetric analysis (TGA) and Fourier transform infrared (FTIR) spectroscopy respectively. The effect of reaction parameters such as methanol to oil ratio (MeOH: Oil), reaction time, reaction temperature, and catalyst concentration on the yield and quality of biodiesel produced was also investigated.

2. MATERIALS AND METHODOLOGY

2.1. Materials

The chemical reagents used in the study were analytical grade (Sigma-Aldrich). These are $Fe(NO_3)_3 \cdot 9H_2O$, $Co(NO_3)_2 \cdot 6H_2O$, $Ni(NO_3)_2 \cdot 6H_2O$, methanol, and *n*-hexane. Other materials which were also purchased include standard bentonite clay, palm kernel oil, distilled water and deionized water. The materials required no further purification.

2.2. Methodology

2.2.1. Preparation of catalyst

The catalyst was synthesized using wet impregnation method. Equal ratio (1:1:1) by wt% of Fe, Co, Ni was considered by weighing 7.23, 4.94, and 4.95 g of their respective nitrate salts, which were dissolved in 50 mL of distilled water and mixed properly. Bentonite clay (8 g) was added to the solution mixture of the three salts. The mixture was allowed to age for 60 min under constant stirring to ensure homogeneity, and the resulting slurry was allowed to dry under ambient conditions before it was dried at a temperature of 120 ℃ for 8 hours. After cooled, the dried sample was ground and screened through a 150 μm sieve size. The fine powder obtained was made to undergo calcination at 500 ℃ for 3 hours to obtain the final catalyst material, Fe-Co-Ni/Bentonite.

2.2.2. Characterization of catalyst

The properties of the synthesized Fe-Co-Ni/Bentonite catalyst were determined using Fourier Transform Infrared (FTIR) to identify functional groups present, High-Resolution Scanning Electron Microscopy/Energy Dispersive Spectroscopy (HRSEM/EDS) to examine its morphology, Thermal Gravimetric Analysis/ Differential Scanning Calorimetry (TGA/DSC) to determine its thermal behaviour and X-Ray Diffraction (XRD) for its crystalline nature.

2.2.3. Heterogeneous trans-esterification reaction

The activity of the Fe-Co-Ni/Bentonite material to be involved in the heterogeneous transesterification reaction between Palm kernel oil (PKO) and methanol was investigated under varying conditions using a Box-Behnken Design: temperature (50, 55, 60 ℃); ratio MeOH: Oil (10:1, 15:1, 20:1); catalyst concentration (5, 10, 15 wt% catalysts to PKO); and reaction time (1, 2, 3 hours). Solvent (*n*-hexane, 5 mL) was used to enhance proper mixing between the oil and methanol. In a typical experiment, PKO (1 g) was preheated, a corresponding quantity of MeOH added and followed by the addition of solvent and catalyst. The reaction was allowed to complete at the desired temperature in a water bath shaker. To effect separation of products, 5 mL of *n*-hexane and 5 mL of distilled water was added and a funnel was used to separate the glycerol (which dissolved in the water phase) from the biodiesel (which dissolved in the *n*-hexane phase). After the h-hexane layer was filtered to remove all trace of catalyst, the mixture was heated to 70 ℃ to get rid of the solvent, leaving only the biodiesel. The yield of biodiesel was obtained using equation (1):

$$\text{Yield} = \frac{\text{Weight of biodiesel}}{\text{Weight of oil}} \times 100\% \quad (1)$$

2.2.4. Characterization and physicochemical properties of biodiesel

To identify compounds present in the biodiesel and their concentrations, GC-MS analysis of biodiesel produced with the Fe-Co-Ni/Bentonite catalyst was carried out. The physicochemical properties of the biodiesel were determined by ASTM standard method. The properties like acid value, free fatty acid (FFA), pour point (ASTM D97), flash point (ASTM D9), cloud point (ASTM D55773), fire point (ASTM D9), and density (ASTM D4052) were determined. The acid value and FFAwere determined according to the ASTM D664 and D5555 respectively. To determine the acid value, 25 mL of diethyl ether was mixed with 25 mL of ethanol and neutralized with 0.1 M NaOH using a few drops of phenolphthalein solution as the indicator. The PKO (10 g) was dissolved in the mixture and titrated against 0.1 M NaOH under continuous shaking until a pink colour, which appears for a few seconds, was obtained. The acid value was obtained using equation (2):

$$\text{Acid value} = \frac{\text{Titre value} \times \text{Normality} \times 56.1}{\text{Weight of oil}} \quad (2)$$

3. RESULTS AND DISCUSSION

3.1. Properties of the Fe-Co-Ni/Bentonite catalyst

The Fe-Ni-Co/Bentonite catalyst prepared as earlier described was characterized for the presence of functional groups, its morphology, thermal behaviour, and crystalline nature using FTIR, HRSEM/EDX, TGA/DSC, and XRD respectively. Presented in Figure 1 is the mid-infrared region (4000-400 cm^{-1}) of the FT-IR spectrum for the synthesised Fe-Co-Ni/Bentonite. The peak at 3626.39 cm^{-1} shows the presence of a Si-OH contributed by the bentonite clay in the catalyst. The peak between 2500 and 2000 cm^{-1} indicates the presence of triple bonds. The peak 1634.83 $cm^{-1}$is due to C=C stretching vibration, C=N stretching vibrations, NO_2 and C=O functional groups, a carboxylic acid salt. The peak at 1479.68 cm^{-1}, 1425.86 cm^{-1} and 1378.36 cm^{-1}shows the presence of C-H deforming vibration. The peak at 1036.41 cm^{-1} indicates the presence of a C-O stretching vibration. The peaks presented at 916.09 cm^{-1}, 871.77 cm^{-1} and 792.61 cm^{-1} are due to the presence of a C-H deforming vibration. The peak at 665.95 cm^{-1} shows C-I stretching vibration. Peaks at 523.48 cm^{-1} and 472.82 cm^{-1} are due to the presence of S-S stretching vibration. The FT-IR result shows that there are traces of silicon compounds, alkynes, alkenes, oximes, nitro compounds, nitrates, nitramine, carboxylic acid, carbohydrates, benzene, iodo-hydrocarbons, and sulphur compounds.

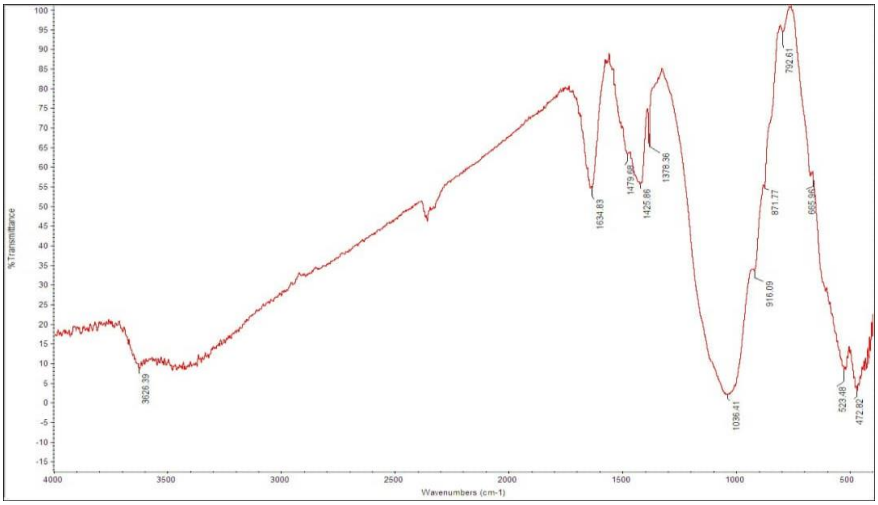

Fig. 1. FT-IR spectrum of Fe-Co-Ni/Bentonite.

The morphology of the catalyst as examined under high-resolution scanning electron microscope is presented in Figure 2.

Figures 2a and 2b showed the same magnification (100x) of the trimetallic catalyst but different sampling points on the sample. While Figure 2c and Figure 2d revealed a reduced magnification (50x) at different sampling points on the sample. The micrographs obtained from HRSEM shows the presence of homogeneously distributed dense and agglomerated plate-like metallic flaky particles on the surface of the support material. It also reveals that the synthesized catalyst is porous, thereby increasing the surface area of the catalyst. The microspore structure of the catalyst provides an adequate external surface that acts as an active site for quick mass transfer in transesterification reactions [20, 21].

Also, the elemental composition was revealed by the energy dispersive X-ray as shown in Figure 3. It confirmed the deposition of Fe-Ni-Co metals on the support material.

The elemental composition of the prepared catalyst was investigated using energy-dispersive spectroscopy. The EDS was recorded in the binding energy region of 0–22 keV as shown in Figure 4. The EDS spectral revealed the presence of C, O, Na, Mg, Al, Si, K, Ca, Fe, Co, Ni and Ba in different proportions. The atomic percentages of C, O, Na, Mg, Al, Si, K, Ca, Fe, Co, Ni and Ba are also shown in Table 2. The percentages of Fe, Ni and Co are relatively small compared to O, C and Si. This can be ascribed to the presence of O, C, and Si in bentonite clay.

The metals Na, Mg, Al, K and Ca were also found in the bentonite clay. The presence of Ba in the catalyst could have come from the bentonite clay source.

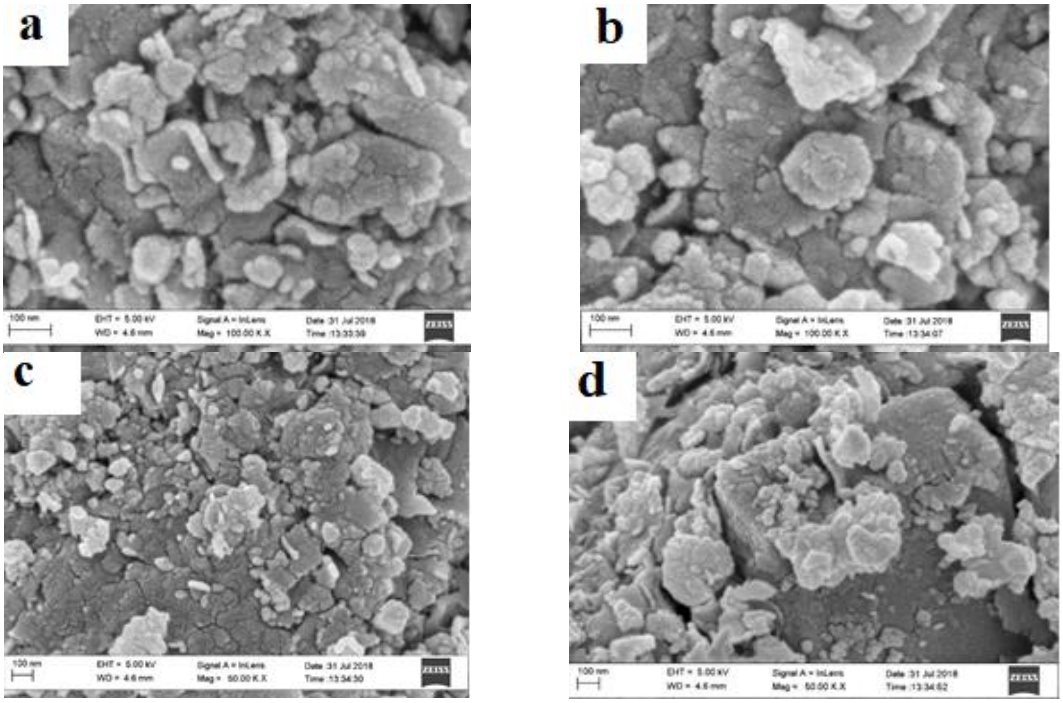

Fig. 2. HRSEM of the bentonite supported trimetallic (Fe–Co–Ni) catalyst:
(a) 100x; (b) 100x; (c) 50x; (d) 50x.

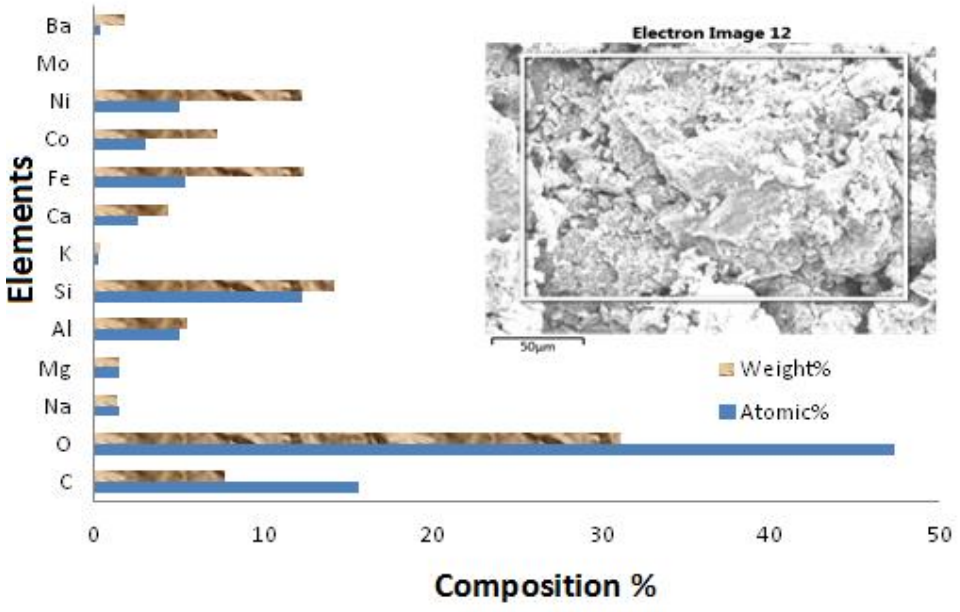

Fig. 3. Elemental composition from EDS of the Fe-Co-Ni/Bentonite.

Table 2. Atomic composition of the synthesized catalyst From EDS spectrum.

Element	C	O	Na	Mg	Al	Si	K	Ca	Fe	Co	Ni	Mo	Ba
Atomic %	15.7	47.36	1.43	1.45	5.0	12.34	0.26	2.64	5.4	3.01	5.1	0	0.32

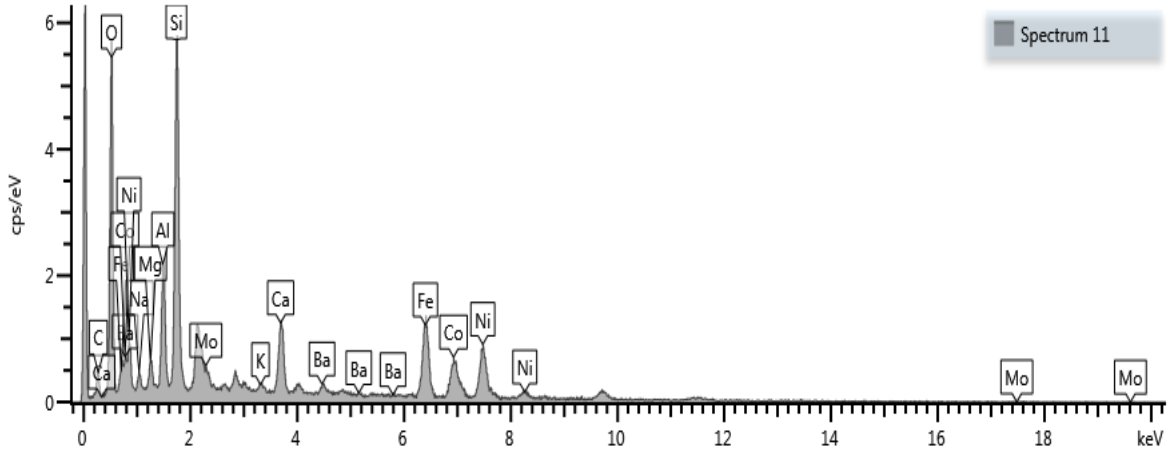

Fig. 4. EDS of the bentonite-supported catalyst.

The thermal stability of the bentonite supported tri-metallic catalyst was investigated using thermal gravimetric analysis (TGA) and differential scanning calorimetry (DSC) curves as presented in Figure 5. The TGA curve shows a weight reduction of 5 % (w/w) at a lower temperature of between 20 and 120 ℃ which can be attributed to the elimination of feasible impurities and desorption of physically absorbed water from the interlamellar region on the surface of bentonite and Fe-Co-Ni trimetallic compound [22]. Further weight loss of 5 % (w/w) was also observed in the temperature range of 120-700 ℃ which can be attributed to the removal of water from the dihydroxylation process [23]. It can also be attributed to the destruction of carbonate which existed in the structure of iron that is present in the nanoparticle [24]. The temperature above 700 ℃ reveals a more stable sample which indicates that the bentonite-supported Fe-Co-Ni trimetallic nanoparticles are a high-temperature-stable catalyst. The DSC profile shows a significant endothermic peak between 20 and 130 ℃, which is related to the removal of free water. The presence of a swelling phase is a reason for the high intensity of the first peak, according to Daroughegi Mofrad et al. [25]. The endothermic peak observed can be assigned to the removal of the interlayer water from the sample.

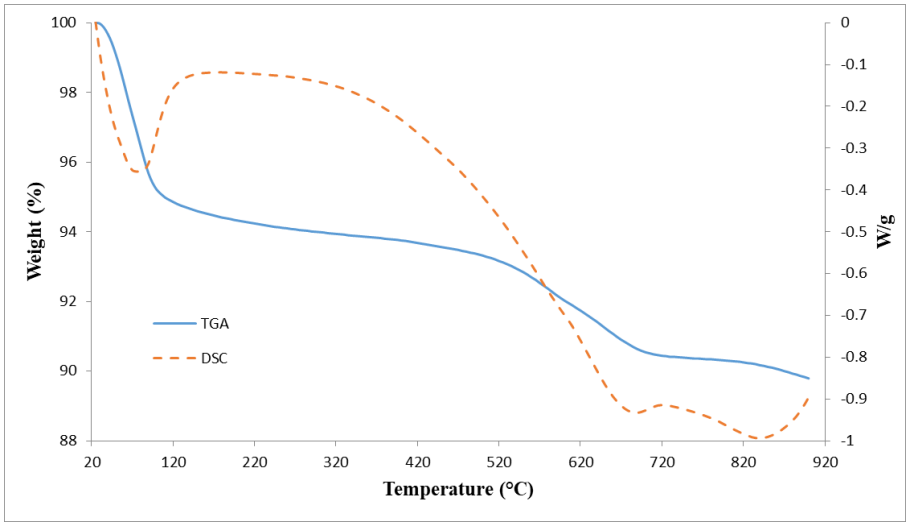

Fig. 5. Thermographic analysis of the developed catalyst.

The XRD pattern of the bentonite supported Fe-Ni-Co catalyst is shown in Figure 6. As observed in the XRD peaks, the synthesized catalyst is crystalline due to the thermal treatment by calcination at a temperature of 500 °C [21]. All the noted peaks on the 2-theta degree: 20.04°, 27.14°, 35.06°, 36.33°, 36.43°, 40.86°, 42.03°, 44.91°, 51.32°, 52.38°, 54.85°, 55.78°, 59.86°, 61.85°, 64.60° and 64.87° represent the peak of Iron oxide hydroxide. A similar result was obtained by Raul *et al.* [26] when they characterize Iron oxide hydroxide.

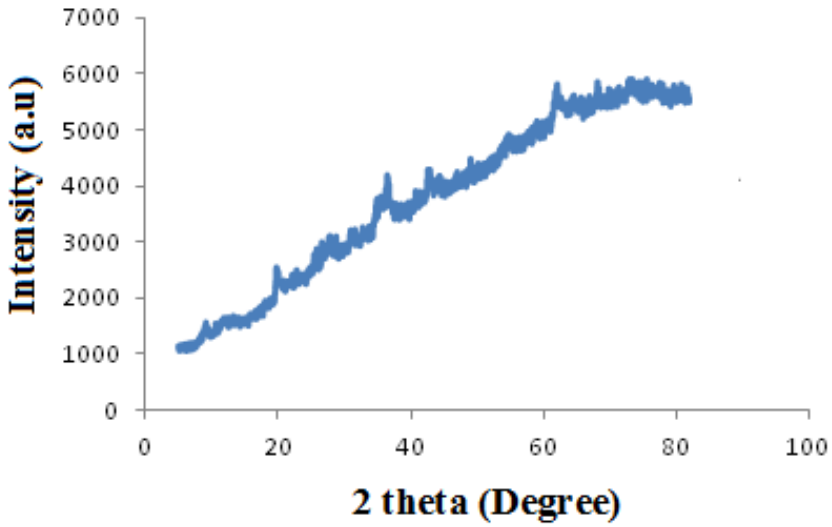

Fig. 6. XRD pattern of the bentonite-supported Fe-Ni-Co catalyst.

3.2. Biodiesel yield and characterization

Using the Box-Behnken design to create the experiment the table was formed. The yield was calculated for every run and was recorded in Table 3.

Table 3. Box-Behnken design of experiment.

Run	MeOH: Oil	Temp (℃)	Time (min)	Cat. Conc. (wt %)	Yield (%)
1	10	50	2	10	81.8
2	15	60	2	5	71.8
3	10	55	2	5	95.2
4	15	55	1	15	87.6
5	15	55	1	5	84.7
6	15	60	2	15	78.6
7	15	60	3	10	68.0
8	10	55	1	10	89.1
9	10	60	2	10	80.9
10	15	50	2	5	82.7
11	15	55	2	10	87.8
12	15	60	1	10	83.6
13	15	55	2	10	82.0
14	10	55	2	15	72.0
15	15	55	2	10	90.3
16	15	55	3	5	90.3
17	15	50	3	10	65.4
18	10	55	3	10	88.5
19	15	55	3	15	90.7
20	15	50	1	10	77.3
21	15	50	2	15	62.2
22	20	55	3	10	89.3
23	20	60	2	10	63.0
24	20	50	2	10	61.1
25	20	55	2	15	75.4
26	20	55	1	10	90.2
27	20	55	2	5	91.4

3.2.1. Effect of temperature and methanol: oil ratio on biodiesel yield. SHA-C

From Figure 7, at a reaction time of 2 hours and catalyst concentration of 10 weight%, it can be explained that the MeOH: Oil ratio has little or no effect on the yield of biodiesel. At a specific MeOH: Oil ratio, the yield increases as the temperature was increased. This yield later experiences a drastic decrease as the temperature was increased above about 55 °C.

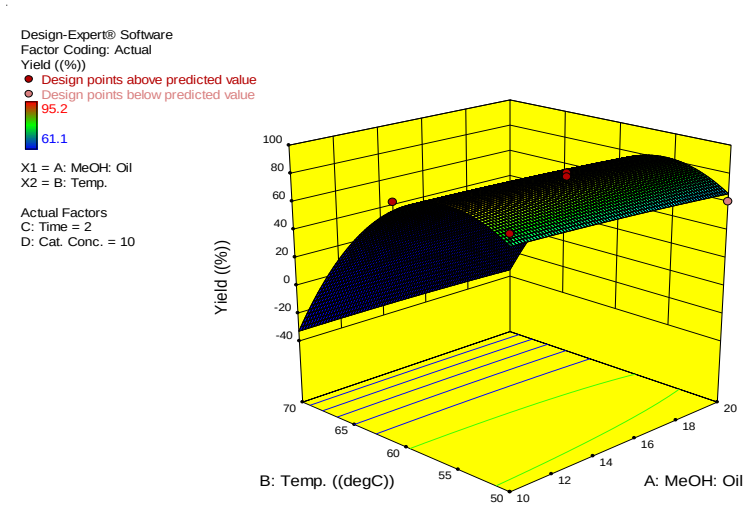

Fig. 7. The effect of temperature and MeOH:Oil ratio on biodiesel yield.

3.2.2. Effect of time and MeOH:oil ratio on biodiesel yield

As shown in Figure 8, at a reaction temperature of 60 °C and catalyst concentration of 10 % weight, the effect of MeOH:Oil and time was presented. A slight reduction in biodiesel yield was observed with an increase in both MeOH:Oil and time.

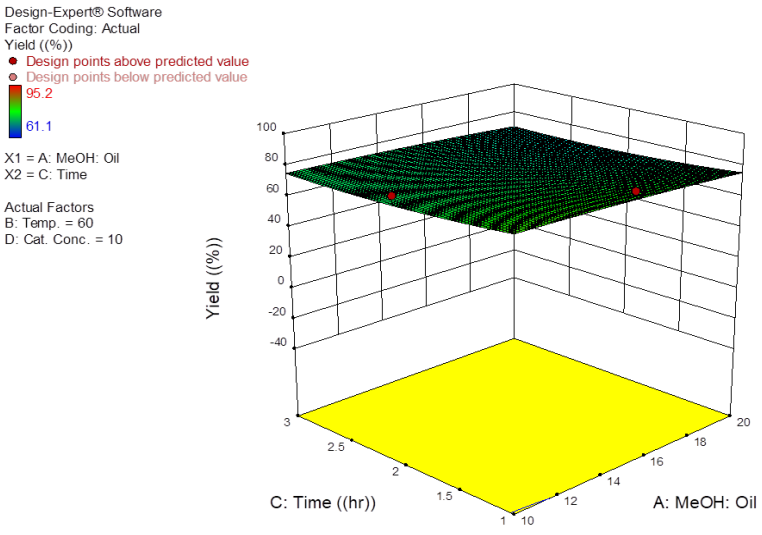

Fig. 8. The effect of time and MeOH:Oil ratio on the yield of biodiesel.

3.2.3. Effect of catalyst concentration and MeOH:oil ratio on biodiesel yield

At reaction temperature of 60 °C and 2 hours in Figure 9, the MeOH:Oil ratio had little or no effect at high catalyst concentrations. At a low catalyst concentration, the biodiesel yield was seen to slightly reduce as MeOH:Oil was increased. Catalyst concentration and MeOH:Oil ratio has the highest effect at a low MeOH:Oil and high catalyst concentration.

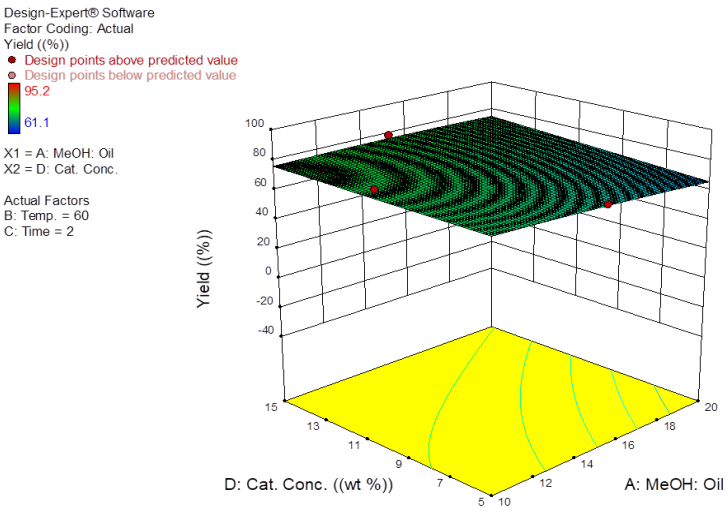

Fig. 9. The effect of catalyst concentration and MeOH:Oil on biodiesel yield.

3.2.4. Effect of time and temperature on biodiesel yield

The effect of reaction time and temperature, at MeOH:Oil ratio of 15:1 and catalyst concentration of 10 weight % is shown in Figure 10. The reaction time alone was found to have a slight effect on yield at low temperature and a more significant effect at high temperature. At any reaction time, the yield of biodiesel increased as temperature increased. The highest yield was found at about 55 °C and at a low reaction time.

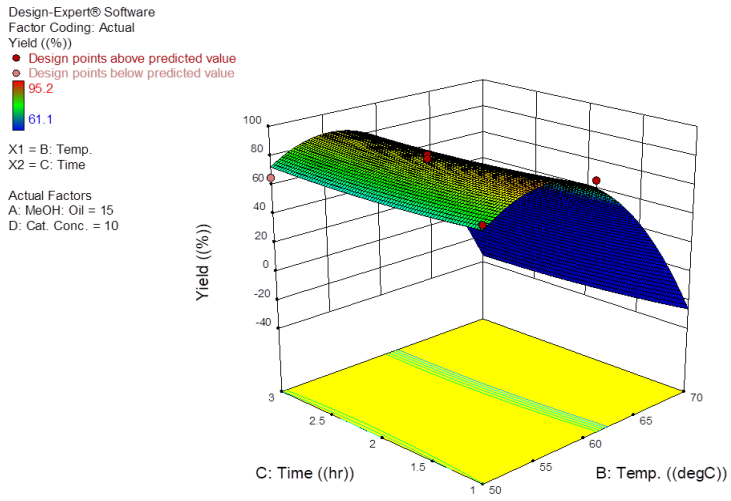

Fig. 10. The effect of time and temperature on biodiesel yield.

3.2.5. Effect of catalyst concentration and temperature on biodiesel yield

Catalyst concentration and time, at MeOH:Oil of 15:1 and 2 hours, both influences the yield as revealed in Figure 11. As catalyst concentration was increased at a low temperature, yield decreased significantly but at a high temperature, yield increased with an increase in catalyst concentration. The reaction temperature also had an effect on the yield of biodiesel. At a low and high catalyst concentration, the effect of temperature was seen to be the same. As the temperature increased from 50 °C, the yield also increased until it reached about 55 °C, after which a decrease in yield was observed. The decrease was more obvious at a low catalyst concentration compared to higher concentrations.

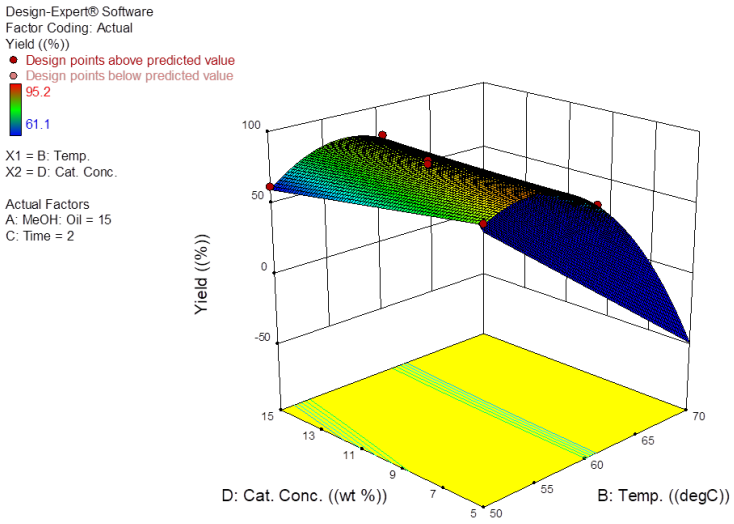

Fig. 11. The effect of catalyst concentration and temperature on biodiesel yield.

3.2.6. Effect of catalyst concentration and time on biodiesel yield

Figure 12 showed that at the reaction temperature of 60 ℃ and MeOH:Oil of 15:1, change in catalyst concentration had little or no effect on yield at any reaction time. At low catalyst concentration, the biodiesel yield was seen to slightly reduce as time increased. Catalyst concentration and reaction time had the highest effect at a low reaction time and high catalyst concentration.

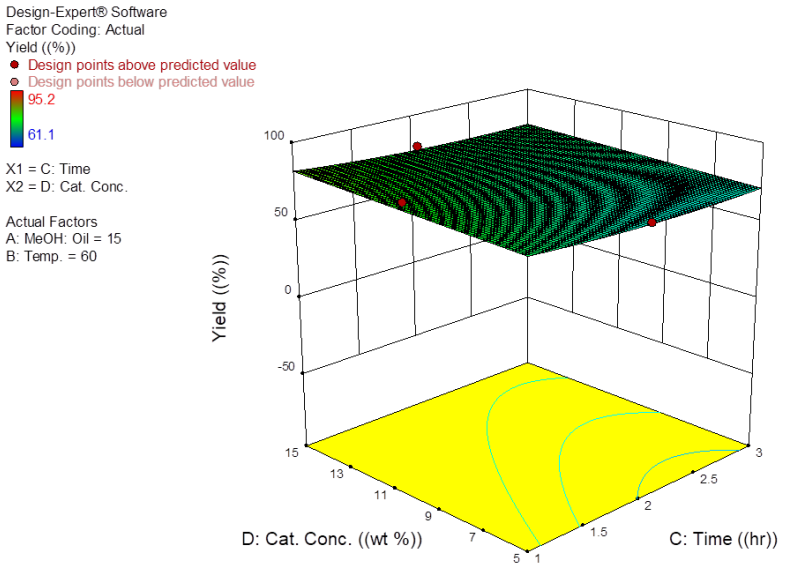

Fig. 12. The effect of catalyst concentration and time on biodiesel yield.

3.2.7. Analysis of variance (ANOVA) for response surface quadratic model

The statistical significance of the designs was confirmed by the analysis of variance (ANOVA) for the response surface quadratic model as shown in Table 4.

The Model's F-value of 2.59 implies this model is significant. There is only a 4.93 % chance that an F-value this large could occur due to noise. The Lack of Fit's F-value of 3.55 implies that it is not significant, relative to the pure error.

Table 4. Analysis of variance (ANOVA) (Partial sums of square-Type III).

Source	Sum of Squares	df	Mean Square	F value	p-value (Prob>F)
Model	1924.12	13	148.01	2.59	0.0493
A-MeOH: Oil	17.16	1	17.16	0.30	0.5932
B-Temp.	902.10	1	902.10	15.77	0.0016
C-Time	20.54	1	20.54	0.36	0.5594
D-Cat. Conc.	21.74	1	21.74	0.38	0.5483
AB	1.96	1	1.96	0.034	0.8560
AC	0.023	1	0.023	3.932E-004	0.9845
AD	12.96	1	12.96	0.23	0.6420
BC	3.42	1	3.42	0.060	0.8106
BD	186.32	1	186.32	3.26	0.0943
CD	1.56	1	1.56	0.027	0.8713
A^2	5.53	1	5.53	0.097	0.7609
B^2	1117.48	1	1117.48	19.53	0.0007
C^2	34.28	1	34.28	0.60	0.4528
Residual	743.81	13	57.22	-	-
Lack of Fit	707.55	11	64.32	3.55	0.2403
Pure Error	36.26	2	18.13	-	-
Cor Total	2667.93	26	-	-	-

There is a 24.03 % chance that a Lack of Fit F-value this large could occur due to noise. A non-significant lack of fit is good. A, B, C and D are the coded values of independent factors methanol to oil molar ratio, temperature, time and catalyst concentration (wt. % of oil) respectively. Values of "Prob > F" less than 0.0500 indicate model terms are significant and value greater than 0.1000 indicates the model terms are not significant. In this case, temperature (B) and temperature^2 (B^2) are the only significant model terms. The ANOVA analysis stipulated the significance of the quadratic polynomial equation for actual variables equation (3).

$$\begin{aligned}\text{Yield} = {} & -1396.62824 - (1.69667 \text{ x Methanol to oil ratio}) + (57.52444 \text{ x Temperature}) \\ & + (0.39722 \text{ x Time}) - (16.67167 \text{ x Catalyst Concentration}) \\ & + (0.028000 \text{ x Methanol to Oil ratio x Temperature}) \\ & - (0.015000 \text{ x Methanol to Oil ratio x Time}) \\ & + (0.072000 \text{ x Methanol to Oil x Catalyst Concentration}) \\ & - (0.18500 \text{ x Temperature x Time}) \\ & + (0.27300 \text{ x Temperature x Catalyst Concentration}) \\ & - (0.12500 \text{ x Time x Catalyst Concentration}) - 0.038389\ (\text{Methanol Oil ratio})^2 \\ & - 0.54589\ (\text{Temperature})^2 + 2.39028\ (\text{Time})^2\end{aligned} \quad (3)$$

The above equation can be used to make predictions about the response for given levels of each factor. Here, the levels should be specified in the original units for each factor. The equation cannot be used to determine the relative impact of each factor because the coefficients are scaled to accommodate the units of each factor and the intercept is not at the center of the design space. In the heterogeneous trans-esterification reactions conducted using the synthesized Fe-Co-Ni/Bentonite catalyst, via Box-Behnken Design, the highest yield of 95.2 % was obtained at conditions of MeOH to Oil ratio of 10, temperature of 55 °C, reaction time of 2 hours, and 5 wt % catalyst concentration.

3.3. Gas chromatography-mass spectrometry (GC-MS)

GC-MS was done on the produced biodiesel to determine its components and the amount of fatty acid methyl esters (FAME) present therein (Table 5). The fatty acid profile consists of 68.22 % unsaturated and 31.78 % saturated fatty acids.

The presence of unsaturated fatty acids produced a biodiesel fuel that has a higher density but lower viscosity, lower cetane number and lower thermal efficiency that emits lower HC, CO and smoke emissions compared to highly saturated biodiesel fuels [1]. Oleic acid fatty ester has the highest % composition in biodiesel with 57.87 %. The total FAME present is 100 %.

Table 5. FAMEs profile and quantitative analysis of biodiesel.

Peak no.	Retention time [min]	FAMEs present	Molecular formula	% Composition
1	20.888	Cyclohexasiloxane, dodecamethyl AN: Cyclomethicone 6	$C_{12}H_{36}0_6Si_6$ Sat	13.56
2	25.227	Hexasiloxane, 1,1,3,3,5,5,7,7,9,9,11,11-dodecamethyl-	$C_{12}H_{36}O_5Si_6$ Sat	15.14
3	29.114	Benzoic acid, 2,5-bis (trimethylsiloxy)-, trimethylsilyl ester	$C_{16}H_{30}O_4Si_3$ Unsat	10.35
4	32.491	Cyclononasiloxane, octadecamethyl- AN: octadecamethylcyclononasiloxane	$C_{18}H_{54}O_9Si_9$ Sat	3.08
5	38.737	Oleic acid	$C_{18}H_{34}0_2$ Unsat	57.87

AN: Another name; Unsat: unsaturated; Sat: saturated

3.4. Physicochemical properties

The physicochemical properties of the biodiesel were obtained and compared to the ASTM standard as shown in Table 6. The results show that all the investigated fuel properties for the palm kernel biodiesel fell between the ASTM standard values for biodiesel production. This is an indication of the conversion of the oil to methyl esters.

Table 6. Fuel properties of palm kernel biodiesel.

S/N	Fuel properties [units]	Palm Kernel Oil biodiesel	ASTM standard for biodiesel	ASTM method
1	FAME content [% m/m]	100 %	≥96.5 %	–
2	Specific gravity	0.866	–	–
3	Density at 15 ^oC [kg/m^3]	866	860 to 900	ASTM D1298
4	Pour point [^oC]	1	-15 to 10	ASTM D97
5	Fire point [^oC]	188	≥130	ASTM D92
6	Flash point [^oC]	179	≥130	ASTM D92
7	Acid value [mg KOH/g]	0.1075	≤0.80	ASTM D664
8	Cloud point [^oC]	6	-3 to 12	ASTM D2500

4. CONCLUSION

Heterogeneous catalysis using bentonite-supported Fe-Co-Ni tri-metallic nanoparticles was investigated in a trans-esterification reaction of palm kernel oil to biodiesel. The nano-catalyst was shown to be crystalline, and Fe-Ni-Co active metals were uniformly dispersed on the clay support material. It was found to be suitable to produce biodiesel, giving an optimum yield of 95.2 % at reaction conditions of 10:1 methanol to oil ratio, 5 % catalyst concentration with respect to the weight of oil, reaction temperature of 55 ^oC and reaction time of 2 hours. The physicochemical properties of the biodiesel produced show that it satisfies the ASTM standards. The GC-MS FAME profile further confirms the quality of the biodiesel.

REFERENCES

[1] Gopinath, A., Puhan, S., Nagarajan, G., Effect of biodiesel structural configuration on its ignition quality, International Journal of Energy and Environment, vol. 1, no. 2, 2010, p. 295-306.
[2] Saravanan, S., Nagarajan, G., Rao, G.L.N, Sampath, S., Feasibility study of crude rice bran oil as a diesel substitute in a DI-CI engine without modifications, Energy for Sustainable Development, vol. 11, no. 3, 2007, p. 83-92.
[3] Herzog, A.V., Lipman, T.E., Edwards, J.L., Kammen, D.M., Renewable energy: A viable choice, Environment, vol. 43, no. 10, 2001, p. 8-20.
[4] Alrikabi, N.Kh.M.A., Renewable energy types, Journal of Clean Energy Technologies, vol. 2, no. 1, 2014, p. 61-64.
[5] Gui, M.M., Lee, K., Bhatia, S., Feasibility of edible oil vs. non-edible oil vs. waste edible oil as biodiesel feedstock, Energy, vol. 33, no. 11, 2008, p. 1646-1653.

[6] Zhang, Y., Dube, M.A., McLean, D.D., Kates, M., Biodiesel production from waste cooking oil: 2. Economic assessment and sensitivity analysis, Bioresource Technology, vol. 90, no. 3, 2003, p. 229-240.
[7] Barnwal, B.K., Sharma, M.P., Prospects of biodiesel production from vegetable oils in India, Renewable and Sustainable Energy Reviews, vol. 9, no. 4, 2005, p. 363-378.
[8] Chisti, Y., Biodiesel from microalgae, Biotechnology Advances, vol. 25, no. 3, 2007, p. 294-306.
[9] Tiwari, A.K., Kumar, A., Raheman, H., Biodiesel production from jatropha oil (*Jatropha curcas*) with high free fatty acids: An optimized process, Biomass and Bioenergy, vol. 31, 2007, p. 569-575.
[10] Ramachandran, K., Suganya, T., Gandhi, N.N., Renganathan, S., Recent developments for biodiesel production by ultrasonic assist transesterification using different heterogeneous catalyst: A review, Renewable and Sustainable Energy Reviews, vol. 22, 2013, p. 410-418.
[11] Zabeti, M., Wan Daud, W.M.A., Aroua, M.K., Activity of solid catalysts for biodiesel production: A review, Fuel Processing Technology, vol. 90, no. 6, 2009, p. 770-777.
[12] Aliyu, A., Abdulkareem, A., Kovo, A., Abubakre, O., Tijani, J., Kariim, I., Synthesize multi-walled carbon nanotubes via catalytic chemical vapour deposition method on Fe-Ni bimetallic catalyst supported on kaolin, Carbon Letters, vol. 21, 2017, p. 33-50.
[13] Kariim, I., Abdulkareem, S.A., Abubakre, O.K., Mohammed, I.A., Bankole, M.T., Tijani, J.O., Studies on the suitability of alumina as bimetallic catalyst support for MWCNTs growth in a CVD reactor, Proceeding of 1st International Engineering Conference (IEC2015), Minna, Nigeria, 1-3 September, School of Engineering and Engineering Technology, Federal University of Technology, 2015, p. 296-305.
[14] Albuquerque, M.C.G., Jiménez-Urbistondo, I., Santamaría-González, J., Mérida-Robles, J.M., Moreno-Tost, R., Rodríguez-Castellón, E., Jiménez-López, A., Azevedo, D.C.S., Cavalcante, Jr., C.L., Maireles-Torres, P., CaO supported on mesoporous silicas as basic catalysts for transesterification reactions, Applied Catalysis A: General, vol. 334, no. 1-2, 2008, p. 35-43.
[15] Abdulkareem, A.S., Kariim, I., Bankole, M.T., Tijani, J.O., Abodunrin, T.F., Olu, S.C., Synthesis and characterization of tri-metallic Fe–Co–Ni catalyst supported on $CaCO_3$ for multi-walled carbon nanotubes growth via chemical vapor deposition technique, Arabian Journal for Science and Engineering, vol. 42, no. 10, 2017, p. 4365-4381.
[16] Grim, R.E., Güven, N., Bentonites: geology, mineralogy, properties and uses, Elsevier, Amsterdam, 2011.
[17] Yesiloğlu, Y., Utilization of bentonite as a support material for immobilization of *Candida rugosa* lipase, Process Biochemistry, vol. 40, 2005, p. 2155-2159.
[18] Chitra, P., Venkatachalam, P., Sampathrajan, A., Optimisation of experimental conditions for biodiesel production from alkali-catalysed transesterification of *Jatropha curcus* oil, Energy for Sustainable Development, vol. 9, no. 3, 2005, p. 13-18.
[19] Knothe, G., Steidley, K.R., Kinematic viscosity of biodiesel fuel components and related compounds. Influence of compound structure and comparison to petrodiesel fuel components, Fuel, vol. 84, no. 9, 2005, p. 1059-1065.
[20] Mansir, N., Teo, S.H., Rashid, U., Taufiq-Yap, Y.H., Efficient waste *Gallus domesticus* shell derived calcium-based catalyst for biodiesel production, Fuel, vol. 211, 2018, p. 67-75.
[21] Pang, Y.X., Bao, X., Influence of temperature, ripening time and calcination on the morphology and crystallinity of hydroxyapatite nanoparticles, Journal of the European Ceramic Society, vol. 23, no. 10, 2003, p. 1697-1704.
[22] Bananezhad, B., Islami, M.R., Ghonchepour, E., Mostafavi, H., Tikdari, A.M., Rafiei, H.R., Bentonite clay as an efficient substrate for the synthesis of the super stable and recoverable magnetic nanocomposite of palladium (Fe_3O_4 /Bentonite-Pd), Polyhedron, vol 162, 2019, p. 192-200.
[23] He, S., Muizebelt, I., Heeres, A., Schenk, N.J., Blees, R., Heeres, H.J., Catalytic pyrolysis of crude glycerol over shaped ZSM-5/bentonite catalysts for bio-BTX synthesis, Applied Catalysis B: Environmental, vol. 235, 2018, p. 45-55.
[24] Hajizadeh, Z., Radinekiyan, F., Eivazzadeh-Keihan, R., Maleki., A., Development of novel and green $NiFe_2O_4$/geopolymer nanocatalyst based on bentonite for synthesis of imidazole heterocycles by ultrasonic irradiations, Scientific Reports, vol. 10, no. 1, 2020, art. no.11671.
[25] Daroughegi Mofrad, B., Hayati-Ashtiani, M., Rezaei, M., Preparation of pillared nanoporous bentonite and its application as catalyst support in dry reforming reaction, Asia-Pacific Journal of Chemical Engineering, vol. 13, no. 3, 2018, art. no. 2188.
[26] Raul, P.K., Devi, R.R., Umlong, I.M., Banerjee, S., Singh, L., Purkait, M., Removal of fluoride from water using iron oxide-hydroxide nanoparticles, Journal of Nanoscience and Nanotechnology, vol. 12, no. 5, 2012, p. 3922-3930.